Eur. Phys. J. B **14**, 569–577 (2000)

THE EUROPEAN PHYSICAL JOURNAL B

EDP Sciences

Stochastic resonance in ferromagnetic domain motion

P. Ruszczynski[1,a], L. Schimansky-Geier[1,b], and I. Dikshtein[2]

[1] Institut für Physik, Humboldt Universität zu Berlin, 10115 Berlin, Germany
[2] Institute of Radio-engineering and Electronics, Russian Academy of Sciences, Mokhovaya st. 11, 103907 Moscow, Russia

Received 14 May 1999 and Received in final form 14 October 1999

Abstract. A model for the motion of a single ferromagnetic domain is studied numerically and analytically. A single strip in two dimensions and pinned at two inhomogeneities is considered. We suppose two stable configurations (positively or negatively curved with pinned ends) due to the action of a bistable potential. Further, it is assumed that the domain is driven externally by periodic and noisy magnetic fields. The noise makes the domain able to flip between the two configurations. The small temporally periodic fields synchronize these flippings and the phenomenon of stochastic resonance is observed. The signal to noise ratio of the output is investigated and shows a maximum for a nonvanishing intensity of the applied noise. Its dependency on the stiffness of the domain is studied.

PACS. 05.40.-a Fluctuation phenomena, random processes, noise, and Brownian motion – 85.70.Kh Magnetic thin film devices: magnetic heads (magnetoresistive, inductive, etc.); domain- motion devices, etc.

1 Introduction

In the last two decades, it has been demonstrated that external noise can play a "positive", constructive role in nonequilibrium situations through its interaction with the nonlinearity of a system [1,2]. A quite spectacular example is the case of stochastic resonance (SR) [3,4], in which the signal-to-noise ratio (SNR) of the output of a dynamical system reaches a maximum for a given nonvanishing value of the intensity of the applied noise. This, from the intuitive point of view, surprising phenomenon has been observed experimentally in a great variety of physical (thin magnetic films [5], lasers [6], and so on), chemical and biological (sensory neurons [7,8]) systems. Common to all these examples is that the systems possess a time scale which might be controlled by the applied noise.

Until the present time most research on SR has been focused on zero-dimensional systems. Specifically in magnetic materials, SR in uniaxial ferromagnetic single-domain particles and thin epitaxial iron garnet films driven by noisy and periodic external magnetic fields at the uniform magnetization reversal has been observed [9]. SNR measurements of such systems have been performed and a maximum of SNR has been found.

Considerable recent attention has been concentrated on SR in spatially-distributed systems which are of great interest for practical application of SR in physics and biology. A group of recent studies refers to SR in coupled stochastic elements. The phenomenon of array enhanced SR has been found for both linearly and nonlinearly coupled bistable elements [10,11]. SR for one and two-dimensional Ising models with Glauber dynamics in the oscillating magnetic field has been recently studied [12–14]. The optimal bath temperature and coupling constant where a SNR maximizes have been found. Spatio-temporal SR has been observed in excitable media [15] and based on a Swift-Hohenberg dynamics [16,17]. SR of a domain wall (DW) motion in a one-dimensional nonuniform magnetic media has been studied [18]. This phenomenon can be observed in magnetic nanostructures with a long extension in only one dimension, named nanowires [19,20].

There is a good experimental possibility of registering the stochastic motion of a DW in the magnetic nanostructures by spin-polarized scanning electron microscopy with high spatial resolution [21], already used successfully for investigation of the spin configuration of such structures [22]. The experimental investigation of DW dynamics in a thin epitaxial ferrite-garnet film has been carried out in [5]. The stochastic motion (Barkhausen jumps) of a DW segment between two nearest pinning centers subjected to some periodic and inhomogeneous magnetic fields and noise has been studied, and measurements of SNR have been performed. SNR of the output has shown a clear maximum by increasing the applied noise strength.

In the present work the motion of a single strip domain driven by external deterministic and noisy magnetic fields in an inhomogeneous thin magnetic film is

[a] *Present address*: Uppsala University, The Angstrom Laboratory, Box 534, Uppsala 75121, Sweden
[b] e-mail: alsg@physik.hu-berlin.de

studied. A single strip domain is an important component of magneto-optic recording devices [23]. Nowadays, behaviour of a single domain subjected to deterministic uniform and nonuniform magnetic fields has been investigated intensively [24–27]. A single strip domain is a region of a film limited by parallel domain walls and magnetized against the remainder of the film and the bias field. Such domains can be produced by either the system of orthogonal conductors with current on the surface of epitaxial ferrite-garnet film or a pair of centered electromagnets placed on the two sides of the film [27]. A single domain with free ends is unstable with respect to tightening into a bubble. But, the ends of a domain are able to be fixed in static pinning centers, as, *e.g.*, given by impurities and other defects of a film or the points of the domain intersection with the coil contour [24–27]. Thereby, in the case of two pinned ends the strip domain between them is straight in the presence of an uniform bias field.

We intend to consider stochastic resonance within the motion of a single domain placed in a double-well shaped potential and restricted by two pinning points (Fig. 1). When the noise and the signal are absent the single domain in the bistable potential will be curved and its profile will have one of two equilibrium configurations which minimizes the total energy of the system.

The domain is driven by external noise and a weak periodic external field. For example, an electromagnet coil excited by a signal produced by a noise generator can be of use as a source of noisy magnetic field [5]. Both forces are considered as global actions (time dependent) and do not depend on the position of the domain. "Weak periodic fields" means that the external signal never has a sufficiently large amplitude that the system escapes to the second stable configuration without noise. Otherwise, with the addition of noise the single domain will surmount the barrier between the two equilibrium configurations and switch to the opposite symmetric configuration. Following the predictions of SR we expect that the action of the weak periodic forces on the hopping dynamics of the domain will become most coherent to the periodic driving at an optimal noise level.

2 Ferromagnetic domain motion

Let us consider a single strip domain pinned at the points $x = 0$, $y = 0$ and $x = l$, $y = 0$. The length l is assumed to be large compared with the width w of the front but small with respect to the curvature radius. For this case one can ignore changes of w and of the energy due to deformations of the domain profile besides some geometrical factor. Then, the Lagrangian equation of motion describing the evolution of the strip domain profile $y(x,t)$ can be derived from the Lagrangian function density

$$L\{y(x,t)\} = T - U. \tag{1}$$

Here

$$T = Md_0w\rho\left(\frac{\partial y}{\partial t}\right)^2\sqrt{1+\left(\frac{\partial y}{\partial x}\right)^2}, \tag{2}$$

stands for the kinetic energy density, $U = E_\mathrm{z} + E_\mathrm{m} + E_\mathrm{s}$ is the potential energy density, where M represents the spontaneous magnetization, d_0 is the thickness of the thin film, and $\rho = m/(2Md_0)$, m is the effective mass per unit area of a domain wall. The contributions to U are the Zeeman (E_z), magnetostatic (E_m), and domain wall surface (E_s) energy densities. The Zeeman contribution is

$$E_\mathrm{z} = 2Md_0w(H_\mathrm{b} - H(y,t))\sqrt{1+\left(\frac{\partial y}{\partial x}\right)^2}, \tag{3}$$

where H_b is the temporally constant and spatially uniform biasing field, $H(y,t)$ stands for spatially inhomogeneous, time dependent periodic and noisy magnetic fields.

The second summand of the potential energy density is given by

$$E_\mathrm{m} = 2Md_0wH_\mathrm{m}\sqrt{1+\left(\frac{\partial y}{\partial x}\right)^2} \tag{4}$$

where H_m is the magnetostatic field.

The expression for the magnetostatic energy density of the infinite straight domain E_m [24] is used as $E_\mathrm{m}(w)$ in the case $l \gg w$. Finally, the domain wall surface energy density contribution is

$$E_\mathrm{s} = 2w\sigma\sqrt{1+\left(\frac{\partial y}{\partial x}\right)^2}, \tag{5}$$

where σ is the DW surface energy density. The physics of this term arises from the exchange interaction. In terms (2-5) a geometry factor $\sqrt{1+\left(\frac{\partial y}{\partial x}\right)^2}$ appears in order to replace the energy density for the bow element by the energy density for dx.

Collecting all temporally constant and spatially uniform fields leads to a common parameter

$$H_0 = H_\mathrm{b} + \frac{\sigma}{Md_0} + H_\mathrm{m}, \tag{6}$$

which is a measure for the stiffness of the domain and can be seen as a kind of coupling parameter [23,28]. Later on it will be one of the central values of the analysis.

Now the Lagrange density (1) can be written as

$$L\left(y, \frac{\partial y}{\partial t}, \frac{\partial y}{\partial x}\right) =$$
$$2Md_0w\left[\frac{1}{2}\rho\left(\frac{\partial y}{\partial t}\right)^2 - H_0 + H(y,t)\right]\sqrt{1+\left(\frac{\partial y}{\partial x}\right)^2}\cdot \tag{7}$$

Since it depends on three variables the Lagrangian equation of motion has to be used in the form

$$\frac{\mathrm{d}}{\mathrm{d}t}\frac{\partial L}{\partial(\partial y/\partial t)} - \frac{\partial L}{\partial y} + \frac{\partial}{\partial x}\frac{\partial L}{\partial(\partial y/\partial x)} = -\frac{\partial Q}{\partial(\partial y/\partial t)} \tag{8}$$

with

$$Q\left(\frac{\partial y}{\partial t},\frac{\partial y}{\partial x}\right)=2Md_0w\rho\lambda\left(\frac{\partial y}{\partial t}\right)^2\sqrt{1+\left(\frac{\partial y}{\partial x}\right)^2}, \quad (9)$$

representing a dissipative function with $\lambda=\alpha M/(m\gamma\Delta)$ as the viscous attenuation, α as the Gilbert relaxation constant, Δ as the domain wall width, γ as the gyromagnetic ratio.

In the following the overdamped dynamics only will be considered. Therefore all terms which have their origin in the kinetic energy density will be neglected. For experimental ferrite-garnet films, the effects associated with the kinetic energy are negligibly small for the sinusoidal driving fields at low-frequency $\Omega \ll 70$ MHz [23]. In this case the driving field frequency is well below the resonance frequencies of the domain walls. It is worth noting that the range of low-frequencies is the most interesting for SR observation.

Then, inserting (9) and (7) into the equation of motion (8) leads to the overdamped dynamics

$$2\rho\lambda\frac{\partial y}{\partial t}-\frac{\partial H(y,t)}{\partial y}+\frac{[H(y,t)-H_0]\frac{\partial^2 y}{\partial x^2}}{1+\left(\frac{\partial y}{\partial x}\right)^2}=0. \quad (10)$$

We assume that $H(y,t)$ is the sum of two external fields, one bistable temporally constant contribution $H_1(y)$, and $H_2(y,t)$ standing for the temporally periodic and noisy excitations. We will analyze two possibilities of a bistable inhomogeneity, in detail the two cases

$$H_1^{(1)}(y)=-\frac{a}{2}y^2+\frac{b}{4}y^4, \text{ or } H_1^{(2)}(y)=-\tilde{a}(\tilde{b}|y|-y^2/2) \quad (11)$$

will be studied and, later on, we call them first and second potentials, respectively. The first potential is a sum of parabolic and quartic ones. The second potential corresponds to the combination of gradient and parabolic potentials and has discontinuities in the derivative at $y=0$. Possibly, bistable potentials of such a type can be set up by a spatially nonuniform magnetic field of a system of permanent magnets [29] or an effective field of magnetic microdefects created by the method of synchrotron X-ray lithography [30] or by the laser annealing method [31].

The gradient magnetic field

$$H_2(y,t)=y[A_0\cos(\Omega_s t+\phi)+\sqrt{2D}\xi(t)] \quad (12)$$

consists of a periodic signal field with frequency Ω_s, amplitude A_0 and initial phase ϕ. Later on we will refer to the force generated by that part as signal. The value of ϕ must be treated as a random variable, uniformly distributed over the interval $[0,2\pi]$ [34]. To make the analysis (theory, experiment and numerics) stationary results should be averaged over this initial phase.

The second contribution originates a noisy force and we assume Gaussian white noise with mean value 0 and autocorrelation function

$$\langle\xi(t)\rangle=0, \quad \langle\xi(t)\xi(t+\tau)\rangle=\delta(\tau). \quad (13)$$

D scales the intensity of this noise. The noise will be of "global" type, *i.e.* it depends like the signal on time only and will have the same value for all $y(x)$. As it can be seen below the noise occurs to be additive *and* multiplicative.

The equation (10) is taken as the basis for a numeric investigation in Section 4 and for a qualitative theory developed in Section 5. Both approaches will evidence stochastic resonance for the motion of the strip and agree qualitatively.

3 The stationary case without temporal forces

An important restriction will be made for the motion of the domain. We assume the domain to be pinned at two points, hence, the following boundary conditions should be obeyed

$$y(x=0)=y(x=l)=0. \quad (14)$$

Then, if $H_2(y,t)=0$, equation (10) possesses the stationary (time independent) solutions

$$y(x)=\pm B\,\mathrm{sn}\left(\frac{x}{x_0},k\right), \quad (15)$$

and

$$y(x)=\pm b\left[1-\frac{\cosh\left(\frac{1}{l_0}(\frac{l}{2}-x)\right)}{\cosh\left(\frac{l}{2l_0}\right)}\right] \quad (16)$$

for the first and second potential, respectively. Here

$$x_0^{-1}=\sqrt{\frac{a+d}{2H_0}}, \quad B=\sqrt{\frac{a-d}{b}}$$
$$k=\sqrt{\frac{a-d}{a+d}}, \quad l_0=\sqrt{\frac{H_0}{a}}, \quad (17)$$

and sn is the elliptic sine, d is a integration constant. Using the condition $\partial y(x)/\partial x=0$ for $x=l/2N, \quad N=1,2,...,$ we can get the equation for the integration constant d for the first potential in the form

$$\frac{l}{2Nx_0}=\mathrm{K}(k), \quad (18)$$

where $\mathrm{K}(k)$ is the complete elliptic integral.

The curve $y(x)$ can have more then one extremum between $x=0$ and $x=l$. Extrema will be at $x=\frac{nl}{2N}$ $(n=1,...,N)$ because of the symmetry of the system. It is evident that the domain configuration with $N=1$ has the minimal energy. Since the curvature of the potential $H_1^{(2)}$ at $y=0$ has a discontinuity in its derivative the curve $y(x)$ has only solutions with one extremum in the case of the second potential.

It follows from (15) and (16) that the domain configuration depends on the stiffness parameters x_0/l or l_0/l for the first and the second potentials, respectively.

The larger H_0 and smaller l and a, the less dangled the domain will become. Approximate expressions of the proposed solutions for stiff and flexible domains can be found in the Appendix A.

Stationary (time independent) configurations of single domains in uniform and inhomogeneous magnetic fields have been studied experimentally in epitaxial garnet-ferrites [24–27]. For the film doped by Bi the parameters are: $4\pi M = 160\,\mathrm{G} = 1.6 \times 10^5\,\mathrm{A/m}$, $\sigma/(4\pi M^2 d_0) = 0.06$, $d_0 = 8.4 \times 10^{-6}\,\mathrm{m}$, $w = 4 \times 10^{-6}\,\mathrm{m}$, $H_0 = 4.4 \times 10^3\,\mathrm{A/m}$, $\alpha = 0.05 - 0.5$, $\gamma = 0.22 \times 10^6\,\mathrm{m/sA}$, $\Delta = 1.0 \times 10^{-6}\,\mathrm{m}$, $\rho\lambda \approx 3 \times 10^4 \ldots 3 \times 10^5\,\mathrm{sA/m^3}$; in inhomogeneous magnetic fields with $\sqrt{a/b} = 2 \times 10^{-6}\,\mathrm{m}$ ($b = 2 \times 10^{-6}\,\mathrm{m}$ and $a = 3.2 \times 10^{13}\,\mathrm{A/m^3}$ for the first potential, and $b = 2 \times 10^{-6}\,\mathrm{m}$ and $a = 0.8 \times 10^{13}\,\mathrm{A/m^3}$ for the second potential), the characteristic length is $l_0 \approx 7.5 \times 10^{-6}\,\mathrm{m}$.

4 Numerical treatment

The domain can be seen in analogy to a stretched spring which is unable to relax into the state corresponding to a straight line $y = 0$. It is due to the action of the attractive forces from the bistable potential $H_1(y)$ above and below the $y = 0$ axis.

Applying additionally temporal noise and temporally periodic forces will drive the "spring" to a flip-flop behaviour between the two stable symmetric configurations. The dynamics of these flippings is dependent on the noise strength and the stiffness of the domain, which will be the main goal of the investigations, later on. The amplitude A_0 of the periodic force is assumed to be sufficiently small that jumps without noise would not occur. Even so we will require that A_0/D will be a small value. Hence, jumps through the energetically unfavourable state $y = 0$ are initiated by the noise but, as will be seen, are synchronized by the periodic signal.

Equation (10) has been simulated by a fast Euler method taking care of the boundary conditions (14). To ensure the reliability of the program the convergence to the stationary (time independent) analytic solution for the potential $H_1^{(2)}$ has been tested and was observed. One of these stationary solutions is marked by the dashed line in Figure 1 and we found agreement with the analytical solution. Figure 1 additionally shows different snapshots of the domain with noise. From the figure one can extract also that the effect of the temporal global noise results approximately in a stochastic change of the elongation of the spring.

Later, in the numeric and theoretical analysis, the stochastic dynamics is further reduced to a two state picture with states $+1$ and -1 depending on the averaged location of the domain above or below the $y = 0$ axis. The response of the system with respect to the noise and the periodic force, later we will call it output $q(t)$, reads, respectively

$$q(t) = \mathrm{sgn}\left(\sum_{i=1}^{n} y(x_i)\right) = \pm 1 \qquad (19)$$

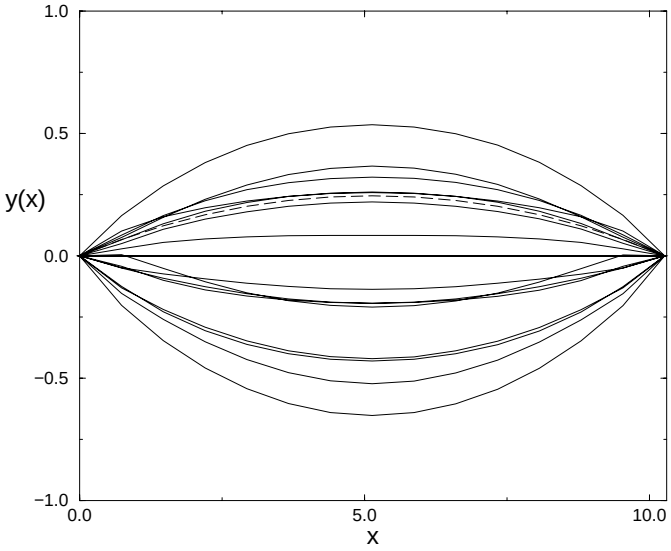

Fig. 1. Example for the flip-flop behaviour of a pinned domain under influence of a global small signal and noise. Different snapshots of stochastic domain configurations from simulations of equation (10) are shown. Approximately, the global forces affect the elongation of the domain. In the absence of noise, a domain is located in one of two stationary (time independent) states. One of them is shown by the dashed lines. A symmetry of the stationary state with respect to replacement of y into $-y$ is restored by noise.

where n is the number of simulated boxes which have been used according to the necessary discretisation of the numerical problem.

The resulting binary time series, *e.g.*,

$$q(t) = ..., +1, +1, -1, +1, -1, -1, -1, +1, ..., \qquad (20)$$

can then be processed by Fourier analysis which has been carried out by a fast Fourier transform (FFT) algorithm. To minimize the errors arising from the FFT aliasing problem a signal frequency Ω_s matching one of the frequencies of the resulting discrete Fourier spectrum has been chosen. The FFT used 4096 sampling points of a total running time of around 2000 time units. A total of 50 spectra with different initial phases had to be averaged in order to get a reasonable stationary power spectrum density (PSD).

The resulting PSD consisting of peaks at Ω_s and its multiples riding on a Lorentzian like background is characteristic of many examples of periodically driven stochastic overdamped nonlinear dynamics. To prove stochastic resonance we have investigated the *signal-to-noise ratio* (SNR) of the output which is given by the weight of the first peak at Ω_s divided by the value of the background noise at this frequency. As shown in Figure 2 the SNR shows a clear maximum while tuning the noise intensity D.

This maximum behaviour is called stochastic resonance. Increasing the intensity of the input noise leads to an increased coherence between the output and the signal. The reason for this behaviour is that tuning the noise intensity leads to a change of the stochastic time scale, the flipping time of the domains. For optimally selected noise

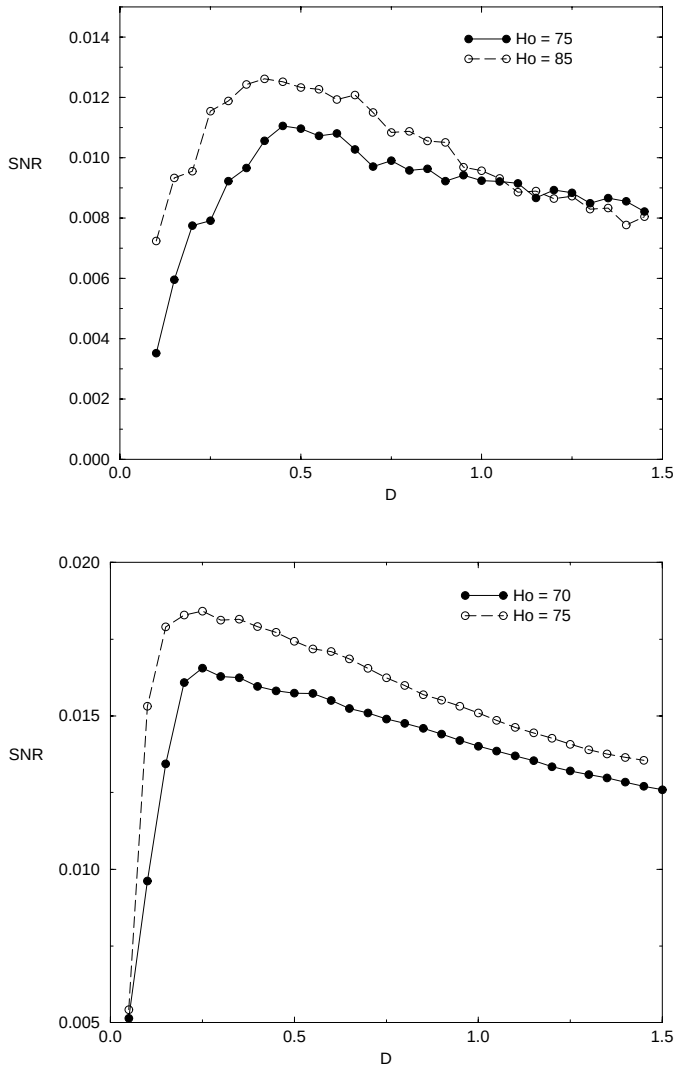

Fig. 2. Maximum behaviour of the signal-to-noise ratio over noise strength D of the simulated motion of the domain in the first (above) and second bistable potentials. Parameters: $\Omega_s = 0.301..$; $A_0 = 0.2$; $l = 11$ resp. 17; $\rho = 1$; $\lambda = 1$; a =12 resp. 2; b =12 resp. 1; $\Delta t = 10^{-3}$; $n = 15$.

this time scale can be brought in accordance with the time of the periodic driving. If the mean time for a single flip equals the half period of the inputting signal the weight of the first peak in the spectrum becomes maximal. It means that a certain amount of flips occurs exactly on the same time scale as the driving signal.

Modern developments of the theory of SR even trace back this phenomenon to a phase synchronization of the output and input [32]. For low noise rare flips occur randomly with a large spread variance, for large noise transitions happen nearly independently of all other acting forces. For optimally selected noise the periodic force is substantial for the dynamics since already small changes of the effective energetic barrier between the two stable configurations influence mainly the temporal behaviour of flipping in accordance with the force or oppositely to it.

On the one side, if the domain is located above $y = 0$ and the periodic force points downwards, the action of this force (despite its smallness) changes the stochastic time scale so far that the stochastic transition to the location below $y = 0$ becomes nearly a sure event within the time the force acts downwards (half period of the signal). The second ingredient is that the probability of re-hopping upwards during that half-period is vanishingly small. Thus the output follows the input during a half period with high probability. Since the situation is symmetric with respect to the change of the force the domain will follow the signal by subsequent changes for sufficiently low frequencies of the driving [33].

Additionally Figure 2 shows that the maximum is shifted to larger values of D if the stiffness parameter H_0 of the domain is decreased. A way to understand this is given in the next section where a qualitative theoretic approach is presented using a picture of an effective potential.

5 Theoretical approach

As the starting point for a qualitative analysis, equation (10) for the overdamped dynamic is used again. Although the approximation $\left(1 + (\frac{\partial y}{\partial x})^2\right)^{-1} \approx 1 - (\frac{\partial y}{\partial x})^2$ for small $\frac{\partial y}{\partial x}$ can be made it is still hard to solve the equation directly. According to Kantarovich [36], the approximate solution of the variational problem should be sought in the form of a finite combination of trial functions with unknown coefficients depending on time. Such an approximation is more adequate for our case than other methods, for example, by means of Ritz's method. As first approximation, the ansatz

$$y(x) = A(t)\left\{B\,\mathrm{sn}\left(\frac{x}{x_0}, k\right)\right\}, \tag{21}$$

$$y(x) = A(t)\left\{b\left[1 - \frac{\cosh\left(\frac{1}{l_0}(\frac{l}{2} - x)\right)}{\cosh\left(\frac{l}{2l_0}\right)}\right]\right\} \tag{22}$$

have been used for the first and second type of bistable potential, respectively.

The motivation to seek solutions in the above given shape is provided by the stationary solution corresponding in both potentials with the factors in (21) and (22) in the brackets. $A(t)$ will represent an elongation of these solutions and equals ± 1 for the stationary case. Also the results of the numerical experiment suggest the usage of this ansatz. Since the second type of bistable potential $H_1^{(2)}$ possesses a discontinuity in its derivative, only qualitative statements can be accepted from this linear approach. The benefit of using this ansatz is that our two-dimensional problem is reduced to a one-dimensional one.

Substituting the ansatzes (21) and (22) into the Lagrangian (1) and dissipative function Q (9) and integrating them with respect to x, we get the functionals $L[A(t)]$ and $Q[A(t)]$. Considering only small deviations of the domain from the $y = 0$ axis, *i.e.* small elongations from $A(t)$ terms, with orders higher than A^4 and A^2, respectively,

for the first and second potential neglected. After carrying out the integration over x this ends up with polynomials in $A(t)$. We get for the first and second potential

$$L^{(1)}[A(t)] = -\left(-\frac{S_1}{2}A^2 + \frac{S_2}{4}A^4\right) + S_3\, A\,[A_0\cos(\Omega_s t+\phi) + \sqrt{2D}\xi(t)], \quad (23)$$

$$Q^{(1)}[A(t)] = (1/2)\Lambda^{(1)}\left(\frac{\partial A}{\partial t}\right)^2, \quad (24)$$

$$L^{(2)}[A(t)] = -\left(-C_1 \mid A \mid + \frac{C_2}{2}A^2\right) + C_3\, A\,[A_0\cos(\Omega_s t+\phi) + \sqrt{2D}\xi(t)], \quad (25)$$

$$Q^{(2)}[A(t)] = (1/2)\Lambda^{(2)}\left(\frac{\partial A}{\partial t}\right)^2. \quad (26)$$

The coefficients $S_1, S_2, S_3, C_1, C_2, C_3, \Lambda^{(1)}$ and $\Lambda^{(2)}$ can be found in the Appendix.

Considering again the overdamped limit (10) of (8) we arrive at the reduced equations for the dynamics of the elongations

$$\dot{A}(t) = \tilde{S}_1 A(t) - \tilde{S}_2 A^3(t) + \tilde{S}_3 A_0\cos(\Omega_s t+\phi) + \tilde{S}_3\sqrt{2D}\xi(t) \quad (27)$$

and

$$\dot{A}(t) = \tilde{C}_1 \mathrm{sign}(A(t)) - \tilde{C}_2 A(t) + \tilde{C}_3 A_0\cos(\Omega_s t+\phi) + \tilde{C}_3\sqrt{2D}\xi(t) \quad (28)$$

with $\tilde{S}_i = S_i/\Lambda^{(1)}$ and $\tilde{C}_i = C_i/\Lambda^{(2)}$.

For $S_1, S_2, C_1, C_2 > 0$ the equations (27) and (28) describe nothing else but the stochastic motion of a Brownian particle in a modulated double well potential with rescaled signal amplitudes $A_{0r}^{(1)} = \tilde{S}_3 A_0$ and $A_{0r}^{(2)} = \tilde{C}_3 A_0$ and with noise intensities $D_r^{(1)} = \tilde{S}_3^2 D$ and $D_r^{(2)} = \tilde{C}_3^2 D$. It is one of the best studied systems in the theory of SR and we are able to use former results by rescaling parameters accordingly to our problem. In particular, we will make use of the theory of McNamara and Wiesenfeld [34] where the dynamics is further reduced to a periodically driven two state random walk in the limit of small amplitudes which is in agreement with the numerical treatment of Section 4. This theory was proven later to give sufficiently good results for small amplitudes [3], especially for a qualitative analysis as in our case.

Two states of elongations $A(t) = \pm 1$ will be considered and rates of transitions for the modified signal amplitudes and noise intensities can be given using standard procedures [35]. Using this Kramers rates for the stochastic processes (27) and (28) the two-state theory of [34] is directly applied. It leads to the calculation of the power spectrum of the two-state output assuming that the power arising from the signal is much smaller than the power of the whole spectrum. Further, to make the analysis independent of the initial state and, hence, transforming the problem into a stationary process, resulting expressions were averaged over a random initial phase of the periodic input (assuming it equally distributed). The resulting power spectrum of this two-state theory consists of two parts, one weighted Fermi-delta function above the signal frequency Ω_s and a continuous Lorentzian-like noise background [3,34].

Therefore the SNR, the ratio of the weight of the delta-function and the noise background at Ω_s, within the described limitations can be determined and we give the expressions for the considered two cases. They read

$$SNR^{(1)} \approx \frac{1}{\sqrt{8}}\,\frac{\tilde{S}_1^2 A_0^2}{\tilde{S}_2\tilde{S}_3^2 D^2}\,\mathrm{e}^{-\frac{\tilde{S}_1^2}{4\tilde{S}_2\tilde{S}_3^2 D}} \quad (29)$$

and

$$SNR^{(2)} \approx \frac{1}{4}\,\frac{\tilde{C}_1^2 A_0^2}{\tilde{C}_2\tilde{C}_3^2 D^2}\,\mathrm{e}^{-\frac{\tilde{C}_1^2}{2\tilde{C}_2\tilde{C}_3^2 D}}, \quad (30)$$

respectively.

The SNRs (29) and (30) are plotted with respect to the noise intensity in Figure 3 and exhibit the well known bell-shaped curves. Qualitatively they agree with the SNR of the numerical treatment and have maxima with values

$$SNR_{\max}^{(1)} = 8\sqrt{8}\,\frac{\tilde{S}_2\tilde{S}_3^2}{e^2\tilde{S}_1^2}\,A_0^2 \quad (31)$$

and

$$SNR_{\max}^{(2)} = 4\frac{\tilde{C}_2\tilde{C}_3^2}{e^2\tilde{C}_1^2}\,A_0^2 \quad (32)$$

located at

$$D_{\max}^{(1)} = \frac{1}{8}\,\frac{\tilde{S}_1^2}{\tilde{S}_2\tilde{S}_3^2} \quad (33)$$

and

$$D_{\max}^{(2)} = \frac{1}{4}\,\frac{\tilde{C}_1^2}{\tilde{C}_2\tilde{C}_3^2} \quad (34)$$

respectively. From the mathematical point of view these maximums are a consequence of the competition of two competing tendencies. On the one side, the noise enters like $\exp(-.../D)$ giving immediately rise to a steep increase with increasing but still small D. For large D this factor is no longer dominating but near 1. In addition, the SNRs have a D dependent prefactor, which depends on a power in D, and thus is unimportant for small D but dominates for D to infinity. It is also clear that in this limit SNR should decrease. Hence, one gets a "maximum", where the strongly increasing small D branch meets the softly decreasing large D branch [3,14].

The calculated SNRs show qualitative agreement with the numerics also in their behaviour for increasing H_0, which stands for the domain stiffness. Both maximums grow and are shifted to lower values of D with increasing stiffness. The coefficients $\tilde{S}_1$, $\tilde{S}_2$ and $\tilde{C}_1$, $\tilde{C}_2$ contain

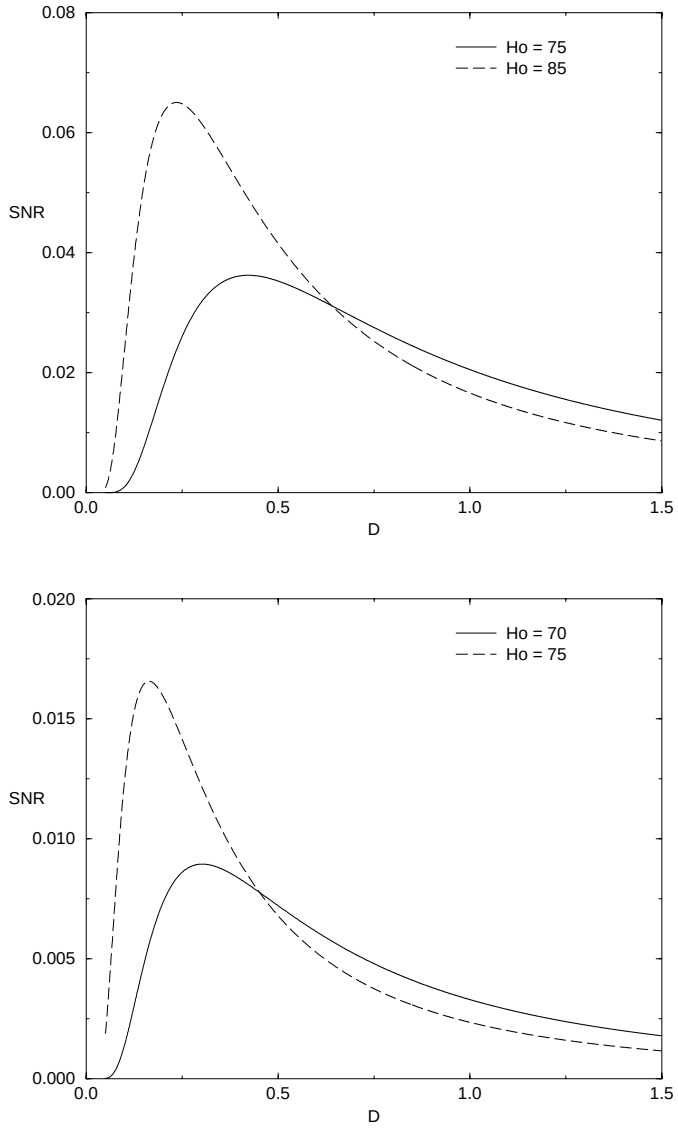

Fig. 3. Maximum behaviour of the analytic signal-to-noise ratio over noise strength D of the motion of the domain in the first (above) and second bistable potentials. Parameters: see Figure 2.

the stiffness parameter x_0/l or l_0/l, respectively. Therefore, the effective potentials for the first and second cases,

$$U_{\text{eff}}^{(1)} = -\frac{S_1}{2}A^2 + \frac{S_2}{4}A^4 \tag{35}$$

and

$$U_{\text{eff}}^{(2)} = -C_1|A| + \frac{C_2}{2}A^2, \tag{36}$$

will change by varying these parameters. An increased parameter x_0/l (or l_0/l) smoothes the effective potentials (35) and (36), the domain is stretched towards the $y = 0$ axis and less noise is needed to bring the domain to the other side of the potential barrier. That explains the growth of the SNR maximum and its shift to lower values of D for an increased stiffness. Therefore our system represents a new example of *array enhanced SR* as discussed in [11–14] but, oppositely, with the shift of the optimal noise to smaller values of D.

We also have to notice the limited agreement of both theory and numerics in the large noise limit. Not only the limited validity of the approximative model but also limits of the numeric algorithm may be responsible for the discrepancy between the theoretical and numerical results (the crossing of the theoretical curves and the noncrossing of the curves of the simulated SNR) for the second type of bistable potential in that region.

6 Conclusions

A noisy magnetic field can enhance the periodic component in the motion of a ferromagnetic domain which is pinned at two inhomogeneities and exposed to a weak periodic signal field. The signal to noise ratio of the output *vs.* input noise intensity shows a maximum which is called stochastic resonance. The position of the maximum is shifted towards smaller noise values if the stiffness of the domain is increased. This is due to the fact that the barriers of the effective potentials (35) and (36) get smaller. The presented effect might be used for a measuring tool for the system's parameters.

Appendix A

A.1 Stiff and flexible domains

The stationary (time independent) solutions (15) and (16) can be substantially simplified in the limiting cases of flexible or stiff domains.

a) In the case of the first potential, we have

$$y(x) = \pm \begin{cases} B \tanh\left(\frac{x}{\tilde{x}_0}\right) & \text{for } 0 < x < l/2 \\ B \tanh\left(\frac{l-x}{\tilde{x}_0}\right) & \text{for } l/2 < x < l, \end{cases} \tag{37}$$

with

$$B = \sqrt{\frac{a}{b}}\left[1 - 4\exp\left(-\frac{l}{\tilde{x}_0}\right)\right] \tag{38}$$

and the other parameters are given by

$$k = 1 - 8\exp\left(-\frac{l}{\tilde{x}_0}\right),$$

$$d = 8a\exp\left(-\frac{l}{\tilde{x}_0}\right),$$

$$x_0 = \tilde{x}_0\left[1 - 4\exp\left(-\frac{l}{\tilde{x}_0}\right)\right]$$

for a flexible domain ($l \gg \tilde{x}_0 \equiv \sqrt{\frac{2H_0}{a}}$) and $N = 1$. For a stiff domain ($l \cong x_{c1} \equiv \pi\sqrt{\frac{H_0}{a}}$) one gets

$$y(x) = \pm B \sin\left(\frac{x}{x_0}\right), \tag{39}$$

with $B = \sqrt{\frac{2a}{b}}k(1-\frac{k^2}{2})$

$$k = \sqrt{\frac{4}{3}\left(\frac{l}{x_{c1}}-1\right)}\left[1-\frac{1}{8}\left(\frac{l}{x_{c1}}-1\right)\right],$$

$$d = a(1-2k^2+2k^4),$$

$$x_0 = \frac{l}{\pi}\left(1-\frac{k^2}{4}-\frac{5}{64}k^4\right).$$

In this case, a domain can become curved for $l \geq x_{c1}$, only. b) In the case of the second potential, the stationary (time independent) solution can be approximated by

$$y(x) = \pm b \begin{cases} \frac{x}{l_0}\left[1-\frac{x}{2l_0}-2\exp\left(-\frac{l}{l_0}\right)\right], \text{ (a)}, \\ 1-\exp\left(-\frac{x}{l_0}\right)-\exp\left(-\frac{l-x}{l_0}\right), \text{ (b)} \\ \frac{l-x}{l_0}\left[1-\frac{l-x}{2l_0}-2\exp\left(-\frac{l}{l_0}\right)\right] \text{ (c)} \end{cases} \tag{40}$$

for a flexible domain ($l \gg l_0$) and where the three cases are for (a): $x < l_0$, (b): $x > l_0$ and $l - x > l_0$ and (c): $l - x < l_0$, respectively. For a stiff domain ($l \ll l_0$) we get

$$y(x) = \pm bx(l-x)/l_0^2. \tag{41}$$

A.2 Coefficients for Section 5

1. For the first potential we have obtained

$$S_1 = \frac{2aB^2l}{3k^2}\left[\frac{2+k^2}{1+k^2}-\frac{4x_0}{l}\mathrm{E}(k)\right],$$

$$S_2 = \frac{bB^4l}{3k^4}\left[2+k^2-\frac{4x_0}{l}(1+k^2)\mathrm{E}(k)\right],$$

$$S_3 = \frac{x_0B}{k}\ln\frac{1+k}{1-k},$$

$$\Lambda^{(1)} = 2\rho\lambda\frac{B^2l}{k^2}\left(1-\frac{2x_0}{l}\mathrm{E}(k)\right)$$

with $\mathrm{E}(k)$ being the complete elliptic function.
2. For the second potential we have obtained

$$C_1 = C_2 = ab^2l\left(1-\frac{2l_0}{l}\tanh\left(\frac{l}{2l_0}\right)\right),$$

$$C_3 = \frac{C_1}{ab},$$

$$\Lambda^{(2)} = 2\rho\lambda b^2l\left(1+\frac{1}{2}\mathrm{sech}^2\left(\frac{l}{2l_0}\right)-\frac{3l_0}{l}\tanh\left(\frac{l}{2l_0}\right)\right).$$

A.3 SNRs in the limit of stiff and flexible domains

With the estimations given in the Appendix corresponding limiting values of the SNR can be estimated. It follows from (31) and (33) that in the large stiffness limit ($l \to x_\mathrm{s}$ or $l \ll l_0$), the maximal values of the SNRs and their corresponding noise intensities behave as $S^{(1)}_{\max} \propto k^{-4} \propto (l/x_\mathrm{s}-1)^{-2}$, $D^{(1)}_{\max} \propto k^4 \propto (l/x_\mathrm{s}-1)^2$ and $S^{(2)}_{\max} \propto (l_0/l)^2$, $D^{(1)}_{\max} \propto (l/l_0)^2$. On the other hand for flexible domains $l/x_0 \to \infty$ or $l/l_0 \to \infty$ the $S^{(1,2)}_{\max}$ and $D^{(1,2)}_{\max}$ approach constants, in particular we have found $S^{(1)}_{\max} = 8\sqrt{2}A^2b/(e^2\rho\lambda a^2)$, $D^{(1)}_{\max} = \rho\lambda a^2/(4b)$ and $S^{(2)}_{\max} = 4A^2/(e^2\rho\lambda ab^2)$, $D^{(2)}_{\max} = \rho\lambda ab^2/2$.

References

1. W. Horsthemke, R. Lefever, *Noise-Induced Transitions* (Springer-Verlag, Berlin, 1984).
2. *Noise in Nonlinear Dynamical Systems*, edited by F. Moss, P.V.E. McClintock (Cambridge University Press, Cambridge, 1989).
3. L. Gammaitoni, P. Hänggi, P. Jung, F. Marchesoni, Rev. Mod. Phys. **70**, 223 (1998); V.S. Anishchenko, A.B. Neiman, F. Moss, L. Schimansky-Geier, Physics-Uspechi **169**, 7 (1999).
4. see: `http://www.pg.infnit/SR/index.html`
5. A.N. Grigorenko, P.I. Nikitin, G.V. Roshchepkin, Zh. Eksp. Teor. Fiz. **112**, 628 (1997).
6. B. McNamara, K. Wiesenfeld, R. Roy, Phys. Rev. Lett. **60**, 262 (1998).
7. F. Moss, Nature **376**, 211 (1995).
8. X. Godivier, F. Chapeaublondeau, Europhys. Lett. **35**, 473 (1996).
9. A.N. Grigorenko, P.I. Nikitin, JETP Lett. **52**, 593 (1990); A.N. Grigorenko, P.I Nikitin, A.N. Slavin, P.Y. Zhou, J. Appl. Phys. **76**, 6335 (1994); A.N. Grigorenko, P.I. Nikitin, Appl. Surf. Sci. **92**, 466 (1996).
10. J. Lindner, B. Meadows, W. Ditto, M. Inchiosa, A. Bulsara, Phys. Rev. Lett. **75**, 3 (1995).
11. A.R. Bulsara, F. Marchesoni, L. Gammaitoni, Phys. Rev. Lett. **76**, 2609 (1996).
12. Z. Neda, Phys. Rev. E **51**, 5315 (1996); Phys. Lett. A **210**, 125 (1996); J. Brey, A. Prados, Phys. Lett. A **216**, 250 (1996).
13. U. Siewert, L. Schimansky-Geier, *Stochastic Dynamics*, edited by L. Schimansky-Geier, T. Pöschel, Ser. Lecture Notes on Physics **486** (Springer-Verlag, Berlin, 1997).
14. U. Siewert, L. Schimansky-Geier, Phys. Rev. E **58**, 2843 (1998).
15. P. Jung, G. Mayer–Kress, Phys. Rev. Lett. **74**, 2130 (1995).
16. J.M.G. Vilar, J.M. Rubi, Phys. Rev. Lett. **78**, 2886 (1997).
17. A.A. Zaikin, L. Schimansky-Geier, Phys. Rev. E **58**, 4355 (1998).
18. I. Dikshtein, A. Neiman, L. Schimansky-Geier, JMMM **188**, 301 (1998); Phys. Lett. A **246**, 259 (1998).
19. F.J. Himpsel *et al.*, Superlattices Microstruct. **15**, 237 (1994); H.J. Elmers *et al.*, Phys. Rev. Lett. **73**, 898 (1994); H.J. Elmers, J. Hauschild, U. Gradmann, *Conference Digest of 15th International Colloquium on Magnetic Films*

and Surfaces (ICMSF'97), 4-8 August (Queensland, Australia, 1997), p. 86.
20. S.A. Gusev, N.A. Korotkova, D.B. Rozenstein, A.A. Fraerman, J. Appl. Phys. **76**, 6671 (1994).
21. K. Koike, H. Matsuyama, K. Hayakawa, Scanning Microsc. Suppl. **1**, 241 (1987); M.R. Scheinfein, J. Unguris, M.H. Kelley, D.T. Piers, R.J. Cellota, Rev. Sci. Instrum. **61**, 2501 (1990).
22. H. Siegmann, J. Phys. Cond. Matter **4**, 8395 (1992); D.P. Pappas, K.-P. Kamper, B.P. Miller, H. Hopster, D.E. Fowler, C.R. Brundle, A.C. Luntz, Z.-X. Shen, Phys. Rev. Lett. **66**, 504 (1991).
23. A.P. Malozemoff, J.C. Slonczewski, *Magnetic Domain Walls in Bubble Material* (Acad. Press, 1979).
24. A.M. Bobeck, Bell System Tech. J. **46**, 1901 (1967).
25. G.J. Zimmer, L. Gal, F.B. Hamphry, J. Appl. Phys. **48**, 362 (1977).
26. V.L. Dorman, V.L. Sobolev, A.L. Sukstanskii, N.E. Shishkova, Sov. Tech. Phys. Lett. **11**, 1058 (1985).
27. V.D. Stasovskii, *Digest of 17th All-Union Conference on Physics of Magnetic Phenomena* (Donetsk, 1985), p. 44.
28. T.H. O'Dell, *Ferromagnetodynamics* (Maximillan Press, 1981).
29. S.V. Gerus, F.V. Lisovskii, E.G. Mansvetova, Sov. Microelectronics **10**, 506 (1981).
30. F. Rousseaux, D. Decanini, F. Carcenac, E. Cambril, M.F. Ravet, C. Chappert, N. Bardou, B. Bartenlian, P. Vallet, J. Vac. Sci. Technol. B **13**, 2787 (1995).
31. J.P. Omaggio, P.E. Wigen, J. Appl. Phys. **50**, 2264 (1979).
32. A. Neiman, A. Silchenko, V. Anishchenko, L. Schimansky-Geier, Phys. Rev. E **58**, 7118 (1998); A. Neiman, L. Schimansky-Geier, F. Moss, B. Shulgin, J.J. Collins, Phys. Rev. E **60**, 284 (1999).
33. The authors of this article are aware of the failing but wide spread usage of the item "resonance" with respect to this phenomenon (see also [3,4]).
34. B. McNamara, K. Wiesenfeld, Phys. Rev. A **39**, 4854 (1989).
35. P. Hänggi, P. Talkner, M. Borkovec, Rev. Mod. Phys. **62**, 251 (1990).
36. L.E. El'sgoltz, *Differential equations and variational calculus* (Nauka, Moscow 1969) in Russian.